Silicon (2022) 14:2573–2581
https://doi.org/10.1007/s12633-021-01016-4

ORIGINAL PAPER

Study the Stability of A 356 Al Alloy/ZrO_2 Composites Fabricated by Vortex and Squeeze Casting in Acid Rain

Awad Sadek Mogoda[1] · Khaled Mohamed Zohdy[2] · Mohamed Ali Aboutabl[1]

Received: 18 October 2020 / Revised: 10 February 2021 / Accepted: 12 February 2021 / Published online: 12 March 2021

Abstract
Electrochemical behavior of A 356 Al alloy and its composites reinforced by zirconia and prepared by vortex and squeeze casting was studied in acid rain using open circuit potential, poteniodynamic polarization, and electrochemical impedance spectroscopy (EIS) techniques. The open circuit potential for the A 356 alloy and its vortex cast composites increases in noble direction very slowly with time till reaches a steady state value indicating growth of the pre-immersion passive oxide film on the tested materials in the acid rain to a certain thickness which increases with increasing of the zirconia content of the composites. Also, the open circuit potential values for the squeeze cast composites are higher than that for vortex composite. This means that the surface of squeeze composite allows for formation passive film with large thickness than that formed on vortex one. The results of polarization and EIS indicated that the corrosion resistance of the vortex composites increases with the increase in the vol. % of ZrO_2 up to 20 % then decreases again. Also, the corrosion resistance of the squeeze composites increases as the squeeze pressure increases. Additional, the micrographs of scanning electron microscopy (SEM) well-showed that the surface of squeeze composite is covered by a passive film and less exposure to corrosion in comparing with the surface of vortex composite. Energy dispersive spectroscopy (EDS) found out the presence of a protective passive aluminium oxide on the two types of the test composites in acid rain.

Keywords A356 Al/ZrO_2 composites · Open circuit potential · Polarization · EIS · SEM · EDS

1 Introduction

Aluminium is the major metal in the A 356 alloys which are very important in automotive and aerospace industry because of light weight, high specific strength, corrosion resistance, modulus, and high thermal conductivity. Metal matrix composites (MMCs) are preferred among the new materials and have high strength and stiffness [1]. Particles reinforced composites exhibit an excellent heat and wear resistance due to superior hardness and heat resistance characteristics of the particles distributed in matrix. These composites are important materials for use in aerospace, automotive and tribological applications because of their higher specific strength and high specific stiffness at room and elevated temperatures.

Aluminium alloy matrix composites (AMC) reinforced with ceramic particles acquire good mechanical properties than unreinforced aluminium alloys [2]. Aluminium matrix composites reinforced with particles, whiskers and ceramic fiber are used as a substitute for steel. The density and compressive strength of AlSiMg (A357) composites containing 10 vol. % ZrO_2 increased while their porosity decreased with increasing squeeze pressure during fabrication [3]. Reinforcing the A 356 Al alloy with ZrO_2 particles increased the hardness and ultimate tensile strength of the alloy produced with 15 vol. % of ZrO_2 at 750 C to the maximum values of 70 BHN and 232 MPa [4]. The addition of alumina (Al_2O_3), titanium dioxide (TiO_2) and zirconia (ZrO_2) nanoparticles as reinforcement agents to the cast aluminum alloy A 356 as a base metal matrix enhanced its mechanical properties [5]. Reinforcing the A 356 Al alloy matrix composite with ZrO_2 resulted in increase of the composite hardness with increasing of the zirconia content and improves the tribological property of the material [6].

✉ Awad Sadek Mogoda
awad_mogoda@hotmail.com

[1] Chemistry Department, Faculty of Science, Cairo University, Giza 12613, Egypt

[2] Higher Technological Institute, Tenth of Ramadan City, Egypt

The corrosion behavior of 6060 and 6082 aluminum alloys in pure water and acid rain is similar, but the aluminum 6060 alloy is more resistant to corrosion in the acid rain than the aluminum 6082 alloy [7, 8]. The electrochemical behavior of aluminium and 8090 Al-Li-Cu-Mg alloy in simulated acid rain (pH 4.5) showed that a protective passive oxide film was formed on aluminium and its alloy at open circuit potential but that formed on the alloy has better protective properties than the film formed on Al [9]. Erosive-corrosive wear behavior of A356 Al alloy and its composite reinforced by ZrO_2 and produced by vortex and squeeze techniques was studied in water containing 40 % sand slurry and the results revealed that the squeezed cast composite is characterized by high corrosion and wear resistance comparing the vortex cast composite [10].

However, studies on the corrosion behavior of A 356 Al alloy / ZrO_2 composites in aqueous solutions are very rarely. In the present wok we compare the corrosion behavior of A 356 Al alloy and its composites reinforced by different vol. % of zirconia and prepared by vortex casting in acid rain. Also, a comparison was made between the vortex composite containing 5 vol. % ZrO_2 and the squeeze casting composites containing the same amount of zirconia and made at different squeeze pressures in the same test solution. The study was carried out using open circuit potential, potentiodynamic polarization and EIS techniques. The morphology and composition of the surfaces of the tested materials were identified by SEM and EDS.

2 Experimental

2.1 Materials

A 356 Al alloy with chemical composition (wt. %) 6.6 Si, 0.5 Fe, 0.34 Cu, 1 Mg and rest Al was used as the matrix alloy. Vortex cast composites were prepared by dispersing different vol. % of ZrO_2 particles with size of 40–100 μm in the matrix alloy using vortex technique. The composite with 5 % ZrO_2 was solidified in a permanent mold using a squeeze casting technique under different pressures namely 20, 50, and 88 MPa [10].

Prior to immersion in the acid rain, the electrodes of test composites were abraded using emery papers with different grades ranging from 600 to 2000 grit, then rubbed with a soft cloth until they acquired a mirror-bright surface and rinsed with distilled water. The chemical composition of simulated acid rain with pH 3.5 is given in Table 1 [7]. All chemicals were Analar grade reagents. The measurements have been achieved in stagnant solution at 25°C.

2.2 Electrochemical Tests

The open circuit potential, EIS, and potentiodynamic polarization measurements were conducted using the electrochemical workstation 1M6e zahner elektrik (GmbH, Meβtechnik, Kronach, Germany) [11–13]. The Echem Analyst software (version 5.21) was used for the electrochemical data analysis. The electrolytic cell was a glass-twofold coat three-electrode cell. A platinum metal was used as an auxiliary electrode. All potentials were measured and reported against saturated calomel electrode (SCE) as a reference electrode. The EIS measurements were performed at open circuit potential. The input signal was usually 10 mV peak to peak in the frequency range from 0.01 Hz to 10^5 Hz. Potentiodynamic scans were traced from − 1.5 to + 0.3 V vs. SCE at a rate of 1 mV s^{-1}.

Table 1 Chemical composition of the simulated acid rain

Material	H_2SO_4	HNO_3	Na_2SO_4	$NaNO_3$	NaCl	$(NH_4)_2SO_4$
g/L water	0.032	0.015	0.0128	0.0084	0.0336	0.0184

2.3 Characterization

The surface morphology of test electrodes were observed by scanning electron microscopy (SEM, Quanta 250 FEG, FEI company, Netherlands). The chemical analysis of electrode surface was performed by energy dispersive X-ray specroscopy (EDS, X Flash detector 4010, Bruker, Germany).

3 Results and Discussion

3.1 Open Circuit Potential Measurements

3.1.1 For A 356 Al Alloy and its Vortex Cast Composites

Variation of the open circuit potential with immersion time in the simulated acid rain for the unreinforced A 356 Al alloy and its vortex cast composites containing different percentages namely 5, 20, and 30 % of ZrO_2 by volume of the alloy, is shown in Fig. 1a. It is clear from this Figure that the open circuit potential for the A 356 alloy and its vortex cast composites increases in noble direction very slowly with time during the period of measurement till reaches a steady state value. The potential at the steady state (corrosion potential) is considered a mixed one, i.e. at this potential the anodic and cathodic processes must be at the same rate on the material surface. The increase of the potential in the positive direction is attributed to the growth of the pre-immersion (air formed) passive oxide film on the tested materials in the acid rain by a dissolution-precipitation mechanism to a certain thickness depending on the zirconia content of these substances. The noble potential value shifts to higher values as the percentage of zirconia in the composites increases up to 20 % then decreases little again at 30 % due to decrease in film thickness as a result

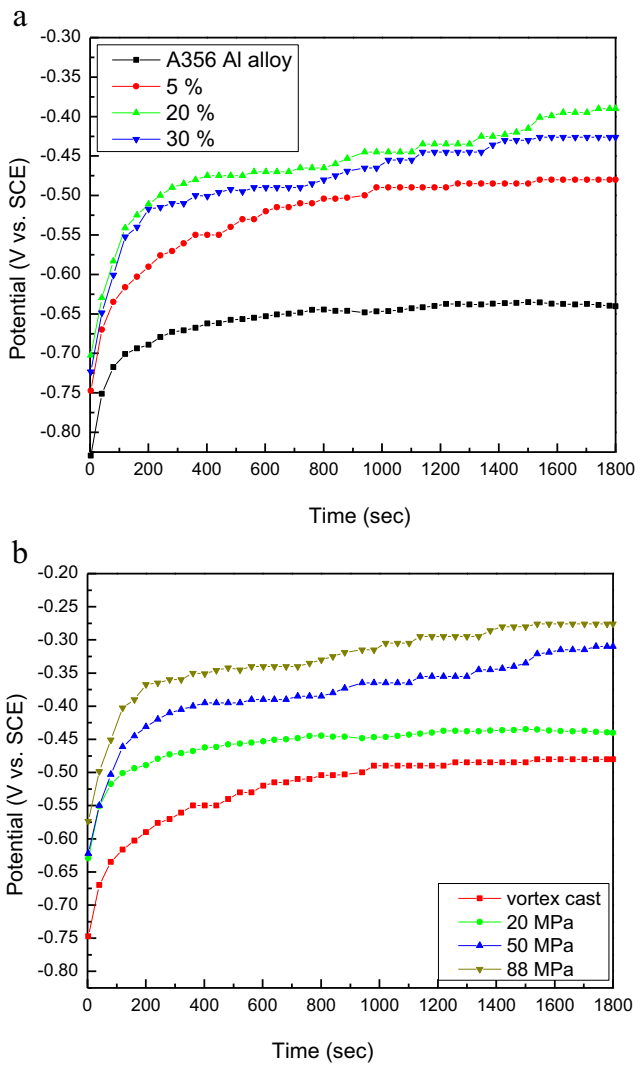

Fig. 1 Variation of the open circuit potential with immersion time in simulated acid rain for (**a**) A 356 Al alloy and its vortex cast composites with different % of ZrO_2 and (**b**) vortex and squeeze cast composites (at different squeeze pressures)

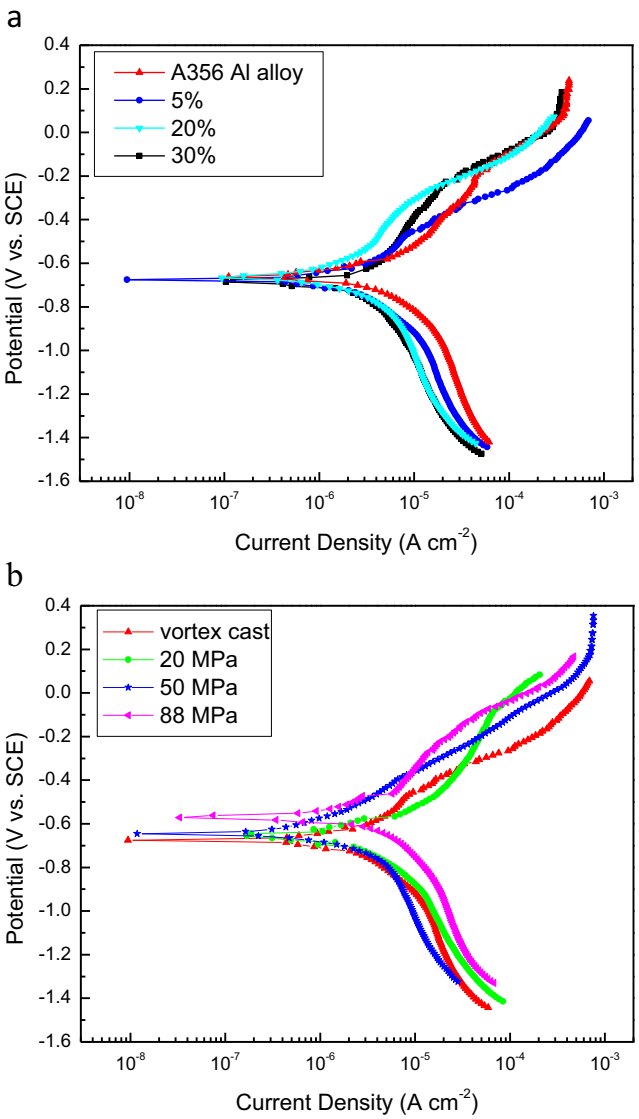

Fig. 2 Potentiodynamic polarization curves in simulated acid rain for (**a**) A 356 Al alloy and its vortex cast composites with different % of ZrO_2 and (**b**) for vortex and squeeze cast composites (at different squeeze pressures)

of its dissolution. This reflects the extent of the improvement of corrosion resistance of these composites with increasing of their ZrO_2 content which helps in repairing and healing of the film existing on the examined materials surfaces. In recently works, we reported that for titanium in fluoride solutions [12] and for bismuth in HCl solutions [13], the open circuit potential got more positive values with time, indicating that the air formed film became thicker.

Previously, it was found that the open circuit potential of Al and 8090 Al-Li-Cu-Mg alloy in acid rain shifts to noble values with time due to formation of a protective passive oxide film on the two materials [9]. The shifting of the open circuit potential to higher noble potential values with immersion time in acid rain for aluminium alloys 6060 and 6082 revealed that those alloys have a lower tendency to corrode in this environment [8].

3.1.2 For Vortex and Squeeze Cast Composites

Variation of the open circuit potential with immersion time in the simulated acid rain for the vortex and squeeze cast composites of A 356 Al alloy reinforced with 5 vol. % of ZrO_2 is given in Fig. 1b. The squeeze composites casting under different pressures namely 20, 50 and 88 MPa. Figure 1b displays that the open circuit potential gets more positive value with time and ends with a steady state value which increases with increasing the casting pressure. Also, the potential values for the squeeze cast composites are higher than that for vortex composite. This means that the surface of squeeze composite allows for formation passive film with large thickness than that formed on vortex one.

Table 2 Potentiodynamic polarization results for A 356 Al alloy and its vortex cast composites with different % of ZrO_2 in simulated acid rain

Vol. % ZrO_2	$E_{corr.}$ mV	$I_{corr.}$ μA/cm^2	Ba mV/ decade	βc mV/ decade	Corrosion rate mpy
0	-685	10.40	1288	1773	8.411
5	-675	3.200	397.2	445.1	2.585
20	-660	2.610	272.0	244.8	2.107
30	-666	2.700	710.2	352.2	2.181

3.2 Potentiodynamic Polarization Measurements

3.2.1 For A 356 Al Alloy and its Vortex Cast Composites

The polarization curves for the unreinforced A356 Al alloy and its vortex cast composites containing different percentages of ZrO_2 in the simulated acid rain are given in Fig. 2a. It is clear from this Figure that the charging curves are characterized by similar cathodic and anodic polarization behavior indicating that the tested samples exhibit the same anodic and cathodic processes. The corrosion parameters were listed in Table 2 and had been analyzed to obtain the following important corrosion parameters: corrosion potential (E_{corr}), corrosion current density (I_{corr}), corrosion rate in mpy, slope of the cathodic branch (β_c) and slope of the anodic branch (β_a).

From the results in Table 2 it is clear that the corrosion potential, $E_{corr,}$ increase in the more noble direction while the corrosion current density, $I_{corr,}$ and consequently the corrosion rate decrease with the increase in the vol. % of ZrO_2 in the vortex cast composites up to 20 %. The addition of ZrO_2 up to 20 % to A356 alloy increases its corrosion resistance but when this content increases to 30 % the corrosion resistance decreases slightly but still very high than the unreinforced A356 alloy. Previously, the potentiodynamic polarization results showed that the corrosion rate of nanocomposite of Al-6061 alloy reinforced with ZrO_2 decreases with the increase in wt. % of n-ZrO_2 in the nanocomposite [14]. The increase of the corrosion resistance of A356 Al alloy with the addition of ZrO_2 particles may be due to these ceramic particles are hardly affected by corrosive medium like acid rain. The efficiency of zirconia added to A 356 Al alloy to improve the corrosion resistance of the resulting composites was calculated on the basis of the corrosion current density. The efficiencies are 69.23, 74.90 and 74.04 % for 5, 20 and 30 % ZrO_2 respectively. This means that the obtained efficiency at 5 % zirconia is large and increases slightly at 20 % then it decreases by very small amount at 30 %.

3.2.2 For Vortex and Squeeze Cast Composites

The polarization curves for the vortex and squeeze cast composites (at different pressures: 20, 50 and 88 MPa) of A 356 Al alloy reinforced with 5 vol. % of ZrO_2 in the simulated acid rain are given in Fig. 2b. It is obvious from this Figure that the polarization curves and passivity characteristics for the vortex and squeeze cast composites are similar. This means the same corrosion processes for the two types of composites tested here. Figure 3a and b shows the SEM micrographs for the mechanically polished surfaces of the vortex cast composite and squeeze cast composite at 50 MPa. It is very clear from this Figure that the pores of different sizes spread in large

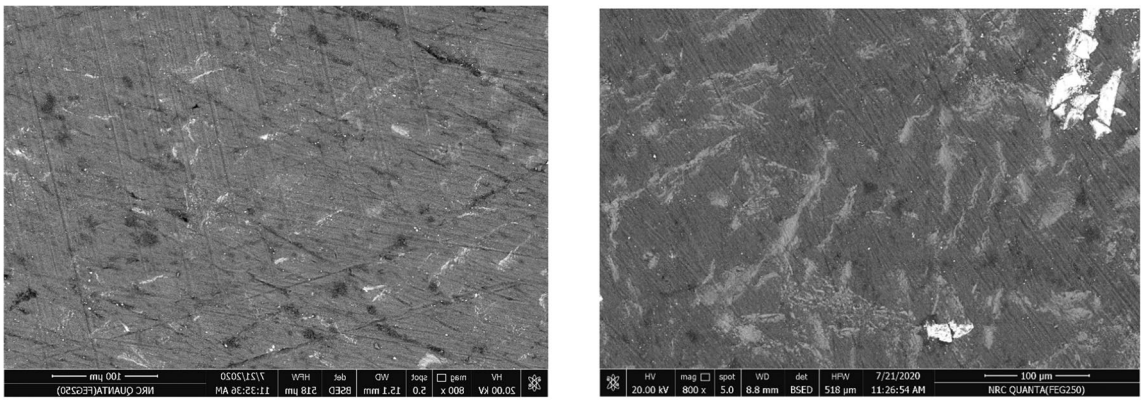

a b

Fig. 3 SEM micrographs for the mechanically polished surfaces of the (**a**) vortex cast composite and (**b**) squeeze cast composite at 50 MPa

Table 3 Potentiodynamic polarization results for vortex and squeeze cast composites (at different squeeze pressures) in simulated acid rain

Squeeze pressure MPa	E_{corr}. mV	I_{corr}. μA/cm^2	Ba mV/ decade	Bc mV/ decade	Corrosion rate mpy
Vortex cast	-675	3.200	397.2	445.1	2.585
20	-652	1.300	155.5	230.2	1.053
50	-645	0.626	227.5	125.1	0.505
88	-570	0.366	98.60	80.30	0.295

amount on the surface of vortex cast composite (Fig. 3a) than on the surface of squeeze one (Fig. 3b).

The polarization parameters were listed in Table 3 in which E_{corr} increases and corrosion rate decreases with increasing of the pressure used for the squeeze composites due to decreasing of their porosity. Also, the values of the corrosion rate for the squeeze composites are lower than that for vortex cast composite of the same percentage of zirconia. Previously, it was found that the values of corrosion current density for A 356/10 vol. % SiC composite cast by gravity are greater than those for composite cast by squeeze in 0.05 and 0.1 M H_2SO_4 solutions [15]. Therefore, squeeze composites are less exposed for corrosion than the vortex one because of their lower porosity content than the vortex composite. Many researchers had been found that the percentage of porosity for the squeeze composite decreases with the increase in the pressure during the preparation process [3, 10, 15, 16].

The efficiency of the squeeze pressure used during fabrication of A 356 Al alloy / 5 vol.% ZrO_2 composite to improve its corrosion resistance was calculated on the basis of the corrosion current density. The efficiencies are 59.38, 80.44 and 88.56 % for 20, 50, 88 MPa, respectively. This means that the efficiency of the squeeze pressure for improvement the corrosion resistance of the squeeze composite increases with increasing the pressure used during casting the composite.

3.3 Electrochemical Impedance Measurements

3.3.1 For A 356 Al Alloy and its Vortex Cast Composites

The EIS spectra have been recorded for the unreinforced A 356 Al alloy and its vortex cast composites containing different percentages namely 5, 20, and 30 % of ZrO_2 in the simulated acid rain at open-circuit potential. The results are shown in Fig. 4a and b as Nyquist plots which are a part of the

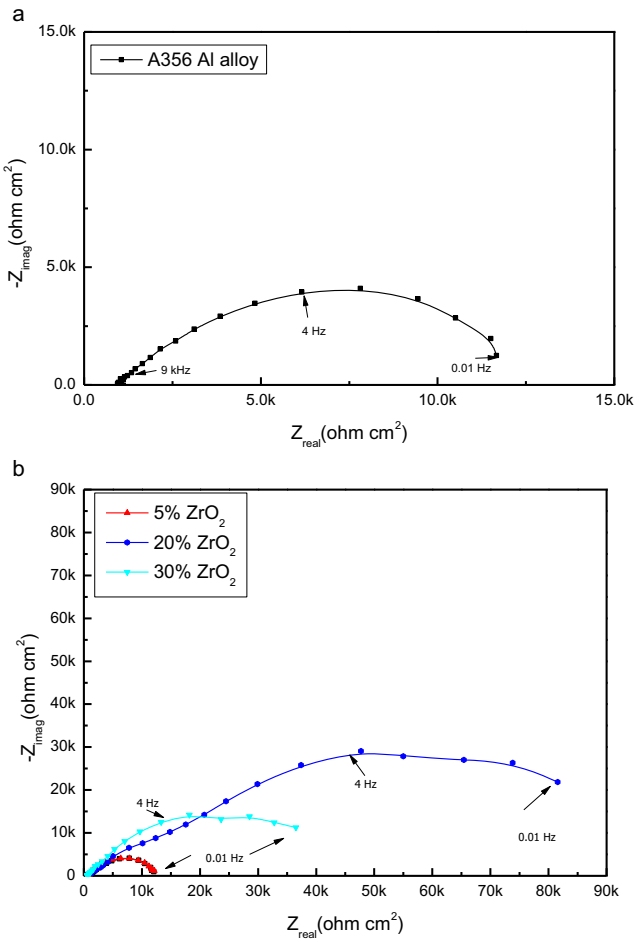

Fig. 4 Nyquist plots for (**a**) A 356 Al alloy and (**b**) its vortex cast composites with different % of ZrO_2 in simulated acid rain

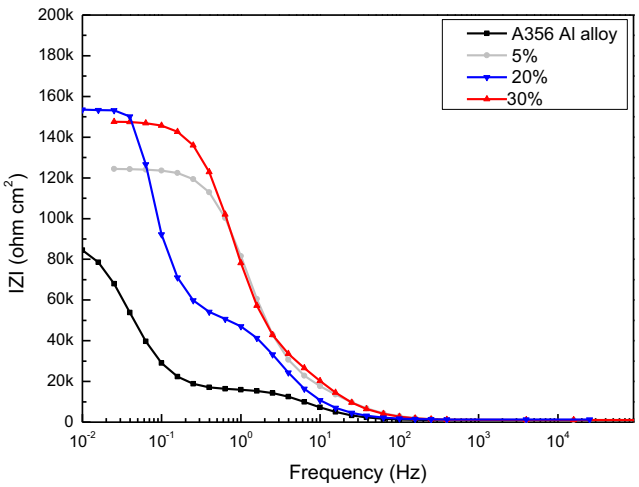

Fig. 5 Bode modulus diagrams for A356 Al alloy and its vortex cast composites with different % of ZrO_2 in simulated acid rain

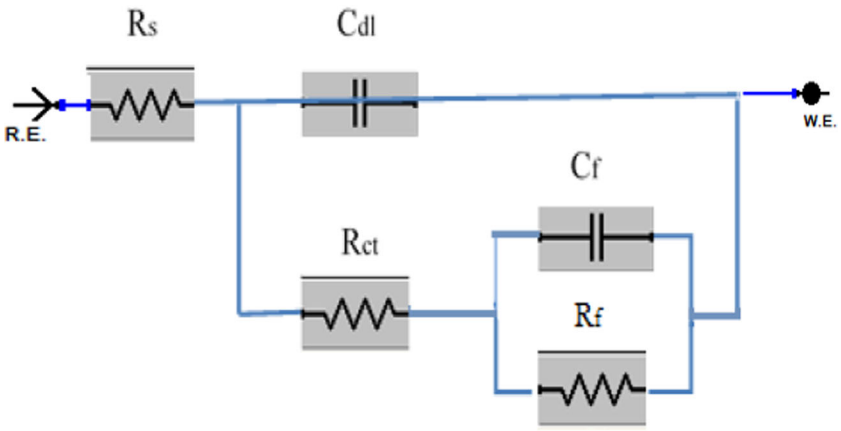

Fig. 6 Equivalent electrical circuit for fitting the impedance data for A356 Al alloy and its vortex and squeeze cast composites in simulated acid rain

imperfect capacitive semicircles due to the frequency dispersion [17]. The capacitive semicircle increases in diameter with increasing the percentage of ZrO_2 added to A 356 Al alloy up to 20 % then decreases again slightly at 30 %. This means that the corrosion resistance of vortex cast composites surfaces in the acid rain increases as ZrO_2 concentration increases up to 20 % then decreases again at 30 %. Also, Fig. 5 shows the variation of impedance as a function of frequency as Bode modulus diagrams [18] for the unreinforced Al alloy and its vortex composites in the acid rain. It is seen from this Figure that the absolute impedance (|Z|) at low frequency increases with the increase in % of ZrO_2 to 20 % then decreases again. The increase in the diameter of capacitive semicircle was observed before for steel in H_2SO_4 solutions containing inhibitors as a result of increasing the corrosion resistance of the steel with increasing the inhibitors contents in the test solutions [19–21].

The impedance data obtained here were analyzed using the equivalent electrical circuit (EEC) in Fig. 6. The components of this EEC are as follows: R_s solution resistance; C_{dl} double layer capacitance; R_{ct} charge transfer resistance that related to the corrosion process; C_f capacitance due to the dielectric nature of the surface film and R_f resistance due to the surface film.

Since there is a variance between real capacitance and pure capacitance therefore, computer simulation of the EIS spectra can be carried out by replacing the capacitance C, with a constant phase element (CPE). The impedance of CPE is described by the following expression [22, 23]:

$$Z_{CPE} = [(j\omega)^{\alpha} Y]^{-1}$$

where Y is the frequency independent real constant of the CPE, ω the angular frequency, $j = \sqrt{-1}$, and α is an adjustable empirical exponent which varies between 1.0 for a perfect smooth surface with pure capacitive behavior and 0.5 for a porous surface.

The fitted EIS parameters for the tested materials in the acid rain were listed in Table 4. It is obvious from this Table that the R_f increases and simultaneously C_f decreases as the percentage of zirconia in the tested composites increases up to 20 % then R_f decrease and C_f increases at 30 %. These variations can be attributed to the increase of the thickness of primary passive film on these materials with zirconia content equals 20 % and decreases when this content equals 30 %.

This can be confirmed from the SEM micrographs in Fig. 7a and b for the surfaces of two vortex composites contain 5 and 20 % zirconia, respectively, immersed for 24 h in acid rain. The composite with 20 % zirconia is covered completely by a homogenous passive film while the other with 5 % zirconia is covered by non-uniform passive film containing big pits. The EDS spectra in Fig. 8a and b conform that the films grew on the two composites consist of aluminium oxide. Recently, it was found that addition of nano silicon carbide particulates ($nSiC_p$) with 1.5 wt. % in the matrix of aluminium alloy 7075 resulted in a decrease in the corrosion rate of the alloy by 39.44 % [24].

Table 4 Characteristic parameters for fitting the experimental EIS results for A 356 Al alloy and its vortex cast composites with different % of ZrO_2 in simulated acid rain

Vol. % ZrO_2	$R_s\Omega$	R_{ct} Ω cm^2	C_{dl} μF cm^{-2}	α_1	R_f Ω cm^2	C_f μF cm^{-2}	α_2
0	988.5	2244	2.39	0.86	8144	79.5	0.79
5	790.8	3377	2.36	0.91	8858	65.4	0.84
20	1000	15,440	2.11	0.89	72,820	43.6	0.75
30	711.9	5117	2.41	0.87	33,570	51.2	0.83

3.3.2 For Vortex and Squeeze Cast Composites

The EIS results for the vertex and squeeze cast composites containing 5 vol. % of ZrO_2 in the acid rain are given in Fig. 9a and b as Nyquist plots. The diameter of the capacitive semicircle increases with the increasing of the casting pressure

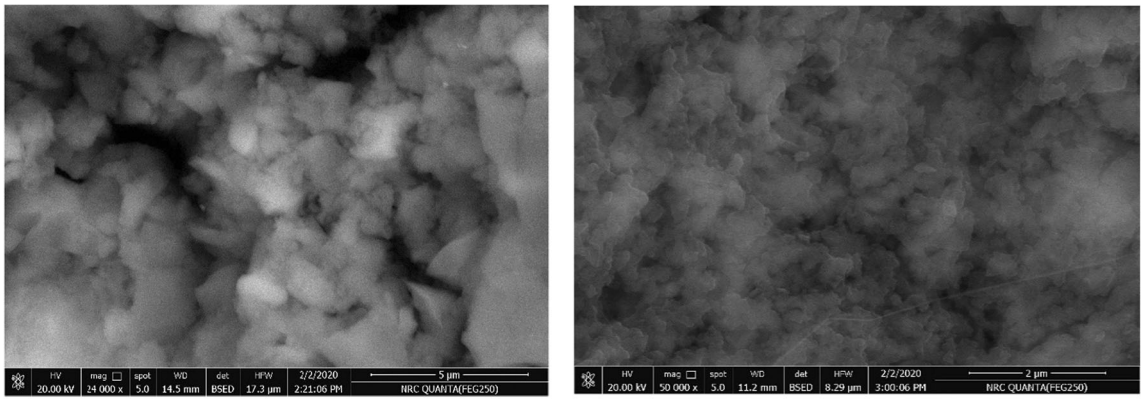

Fig. 7 SEM micrographs for the surfaces of two vortex cast composites contain (**a**) 5 % and (**b**) 20 % zirconia immersed for 24 h in the simulated acid rain

of the composites as a result of improvement of their corrosion resistance. Fitting of EIS results were carried out using the EEC in Fig. 6 and the results are given in Table 5. Both the charge transfer resistance, $R_{ct,}$ and passive film resistance, $R_{f,}$

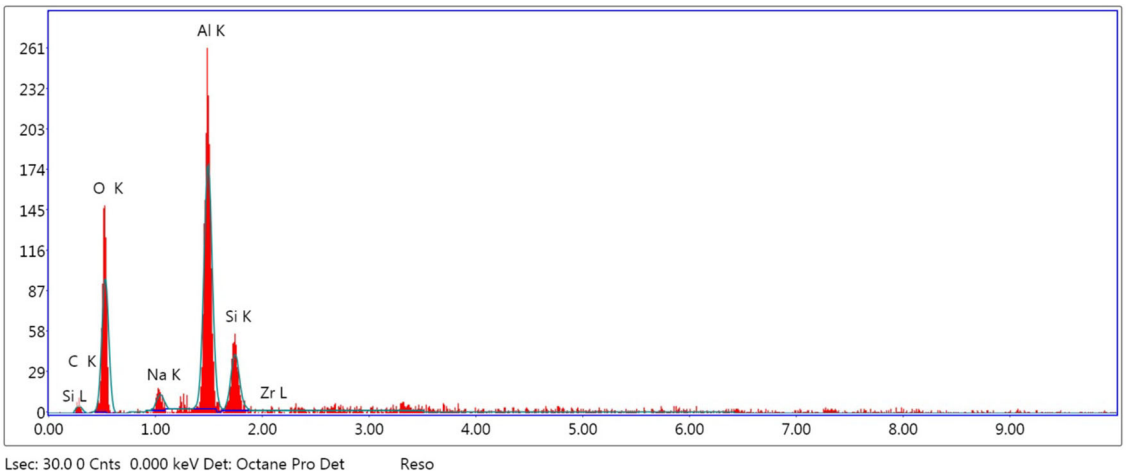

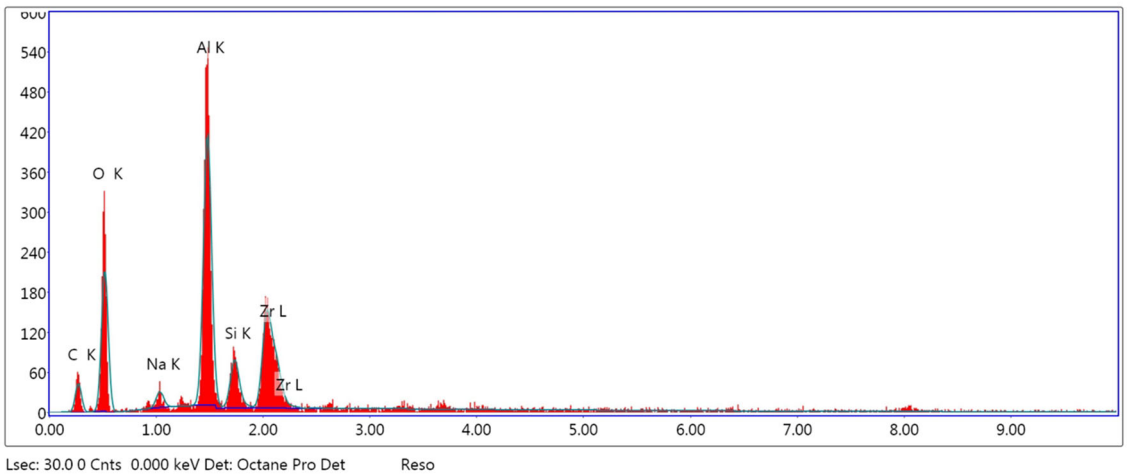

Fig. 8 EDS analysis for the surfaces of two vortex cast composites contain (**a**) 5 % and (**b**) 20 % zirconia immersed for 24 h in the simulated acid rain

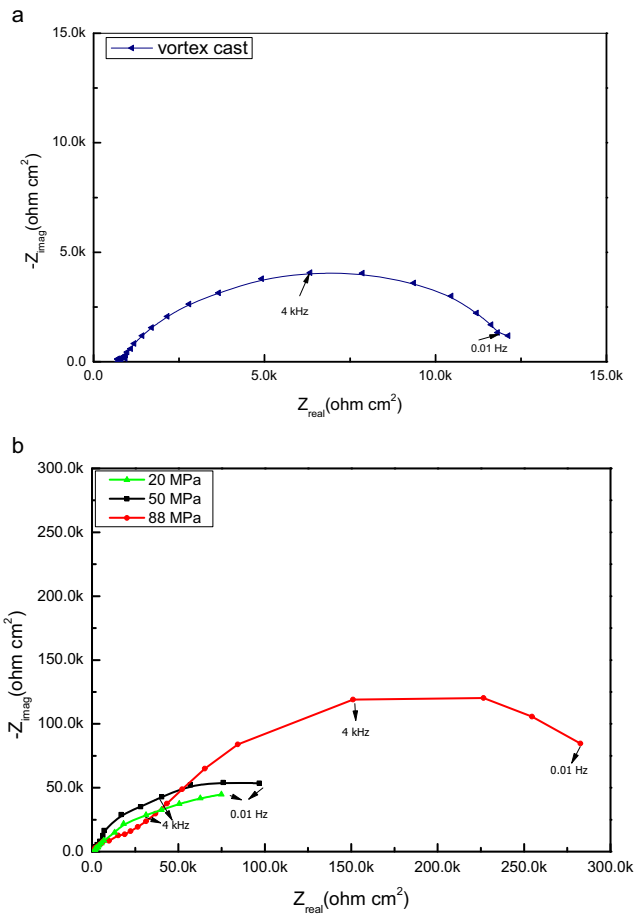

Fig. 9 Nyquist plots for (**a**) vortex and (**b**) squeeze cast composites (at different squeeze pressures) in simulated acid rain

increase as the pressure of squeeze cast composites increases and they are being greater than those of vortex composite. These results are in a reasonable agreement with those obtained by other authors [15].

Figure 10 shows the SEM micrograph for the surface of squeeze composite made at 50 MPa and immersed in the acid rain for 24 h. Comparing this micrograph with that for vortex composite (Fig. 7a) of the same zirconia % we find that the surface of squeeze composite is less exposure for corrosion than the vortex one of high porosity content. Generally, the obtained data here ensured that the squeeze cast alloy has high corrosion resistance in acid rain, which is in a good agreement with Dobrzanski et al. [25].

4 Conclusions

The open circuit potential for A 356 Al alloy and its composites prepared by vortex and squeeze casting techniques increases in noble direction with time indicating growth of the air formed passive film on the tested materials in the acid rain. The shifting of the open circuit potential to the positive direction depends on the zirconia content of the vortex composites and the pressure of squeeze cast composites. The potentiodynamic polarization results revealed that the addition of ZrO_2 up to 20 % to A 356 Al alloy increases its corrosion resistance but when this content increases to 30 % this corrosion resistance decreases slightly but still very high than that of the unreinforced A 356 alloy. Also, the values of the corrosion rate for the squeeze composites are lower than that for vortex cast composite of the same percentage of zirconia. The efficiency of both zirconia and pressure for improvement the corrosion resistance of the composites increases with increasing ZrO_2 content and the casting pressure of these composites.

Moreover, the EIS results reveal that the charge transfer resistance, $R_{ct,}$ and the passive film resistance, $R_{f,}$ increase with increase in the zirconia content in the vertex composites up to 20 % and decrease at 30 % by a little value. These variations can be attributed to the increase of the thickness of primary passive film on these materials to a maximum value at 20 % zirconia. Both R_{ct} and R_f increase as the pressure of squeeze cast composites increases and they are being greater than those of vortex composite. Therefore, the squeeze cast alloys have high corrosion resistance than the vortex cast ones due to the first ones contain low porosity than the vortex ones. The SEM micrographs showed that for the vortex composite contains 20 % ZrO_2 and squeeze one contains 5 % ZrO_2 at 50 MPa protective passive films include much less very minor pits were formed on their surfaces. Additionally, The EDS spectra conformed that the films grew on the vortex and squeeze composites consist of aluminium oxide.

Table 5 Characteristic parameters for fitting the experimental EIS results for vortex and squeeze cast composites (at different squeeze pressures) in simulated acid rain

Squeeze pressure MPa	$R_s\Omega$	R_{ct} Ω cm^2	C_{dl} μF cm^{-2}	α_1	R_f Ω cm^2	C_f μF cm^{-2}	α_2
Vortex cast	790.8	3377	2.36	0.88	8858	65.4	0.81
20	1008	27,060	0.60	0.79	96,390	2.29	0.75
50	1021	41,850	0.55	0.90	104,900	1.98	0.76
88	1317	53,490	0.49	0.94	188,400	1.30	0.71

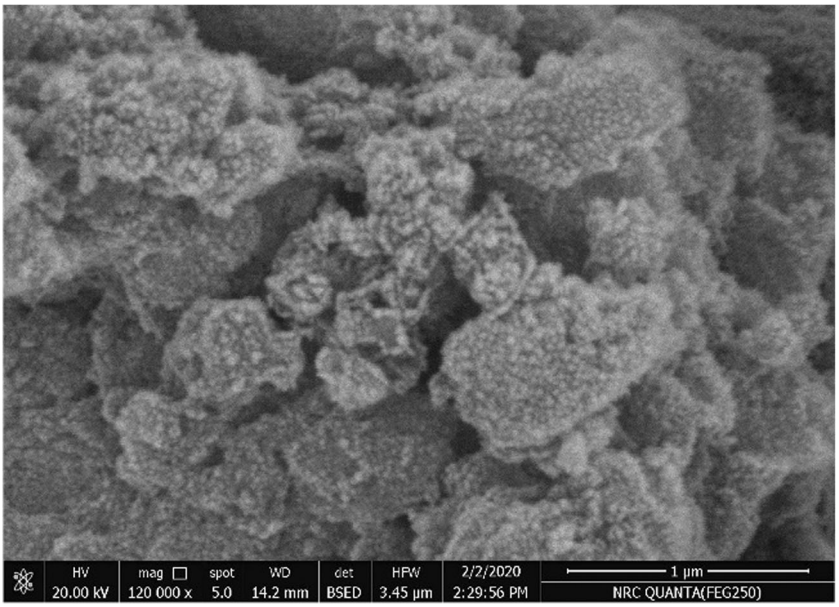

Fig. 10 SEM micrograph for the surface of squeeze cast composite made at 50 MPa and immersed in the simulated acid rain for 24 h

Author Contributions The authors in the present manuscript were contribute in everything and they are accepted by the arrangement of their names as wrote in the paper.

Data Availability The data and material of our work are included in this article.

Declarations

Human and Animal Rights The present article does not contains any studies involving animals or human participants performed by the authors.

Conflict of Interest The authors have no conflict of interest.

Consent to Participate We agree to participate in everything suggested by the Journal.

Consent for Publication All the authors whose names are mentioned in the present manuscript agree for publication in the silicon Journal.

References

1. Suma A, Rao P, Nayak J, Shetty AN (2006) Trans SAEST 41:1
2. Kok M, Ozdin KJ (2007) J Mater Process Technol 183:301
3. El-Khair MTA (2011) Inter J Eng Res Africa 4:59
4. Abdizadeh H, Baghchesara MA (2013) Mech Compos Mater 49: 571
5. El-Mahallawi IS, Shash AY, Amer AE (2015) Metals 5:802
6. Mariyappan M, Sarangapani P, Perumal G, Sathiyamoorthi A (2015) Compos J Chem Pharm Sci 9:98
7. Gerengi H, Slepski P, Ozgan E, Kurtay M (2015) Mater Corros 66:233
8. Gerengi H, Bereket G, Kurtay M (2015) J Taiwan Inst Chem Eng 0:1
9. Pilić Z, Martinović I (2017) Int J Electrochem Sci 12:3576
10. El-Khair MTA, Aal AA (2007) Mater Sci Eng A 454156
11. Mogoda AS, Ahmad YH (2019) Silicon 11:2837–2844
12. Mogoda AS, Zohdy KM (2020) Int J Electrochem Sci 15:8070
13. Mogoda AS (2020) Bull Mater Sci 43:100
14. Ramachandra M, Maruthi GD, Rashmi R (2016) Int J Mater Metall Eng 10:1321
15. Fattah-alhosseini A, Ranjbaran M, Vahid SV (2014) Int J Corros 2014:1
16. El-Khair MTA (2005) Mater Lett 59:894
17. Lebrini M, Lagrenee M, Vezin H, Traisnel M, Bentiss F (2007) Corros Sci 49:2254
18. Sharma Gaurav, Singh K (2021) Silicon https://doi.org/10.1007/s12633-021-00940-9
19. Ahmad YH, Mogoda AS, Gadallh AG (2012) Int J Electrochem Sci 7:4929
20. Sherif El-Sayed M, Abbas A Taha, Halfa Hossam, El-Shamy AM (2015) Int J Electrochem Sci 10:1777
21. Zohdy KM, El-Shamy AM, Kalmouch Atef, Gad Elshafie AM (2019) Egyp J Petrol 28:355
22. Juttner K (1990) Electrochim Acta 35:1501
23. Heakal FE, Ghoneim AA, Mogoda AS, Awad Kh (2011) Corros Sci 53:2728
24. Prakash J, Gopalakannan S, Chakravarthy V. Kalyana (2021) Silicon https://doi.org/10.1007/s12633-021-00979-8
25. Dobrzanski LA, Wlodarczyk A, Adamiak M (2005) J Mater Process Technol 162:27